



Mineralogical and geochemical changes in conglomerate reservoir rocks induced by CO₂ influx at Mihályi-Répcelak natural analogue, NW-Hungary

Viktória Forray¹ · Csilla Király² · Attila Demény³ · Dóra Cseresznyés^{1,4} · Csaba Szabó¹ · György Falus^{1,4}

Received: 10 January 2020 / Accepted: 11 October 2021 / Published online: 8 November 2021
© The Author(s) 2021

Abstract

A temporary solution to massive anthropogenic CO₂ emissions can be the capture of industrial CO₂ from flue gas and sequestering it in geological formations. For safe and effective storage of CO₂, interaction processes in the rock-pore fluid–CO₂ system should be known. Investigation of natural CO₂ accumulations provides valuable examples to what physical and chemical effects could be expected during CO₂ influx at future CO₂ storage sites. One of the key controlling factors of the processes occurring in natural CO₂ reservoirs is the lithology of the storage rocks, which is primarily determined by the formation conditions of these rocks. In this respect, the lithologies of individual CO₂ accumulation areas influence the processes between the host rock, the pore fluid, and the CO₂ in different ways. In the current study, we focus on a well-studied natural CO₂ storage reservoir, namely the Mihályi-Répcelak area, NW Hungary. We provide insight into the so far unstudied conglomerate reservoirs that represent a stratigraphically deeper reservoir unit with significantly different lithology and pore water compositions compared to the sandstone reservoirs. Our results indicate that dawsonite /NaAlCO₃(OH)₂/ formation also affected the conglomerate reservoirs, which indicates that at least part of the CO₂ could be trapped in mineral form. An important role of salinity in reducing the CO₂ mineral trapping capacity of the storage system is also demonstrated. Furthermore, H isotope analysis of diagenetic kaolinite was applied to trace the origin of the pore water that was present during the rock formation. Based on the data, dawsonite formation was induced by the flux of meteoric water that infiltrated during a warm and humid period and mixed with ascending CO₂.

Keywords CO₂ capture and storage · Dawsonite · Natural analogue · Conglomerate reservoir

✉ Csilla Király
kiraly.csilla@csfk.org

- ¹ Lithosphere Fluid Research Lab (LRG), Department of Petrology and Geochemistry, Institute of Geography and Earth Sciences, Eötvös Loránd University, Pázmány Péter u. 1/C, Budapest 1117, Hungary
- ² Geographical Institute, Research Centre for Astronomy and Earth Sciences, Budaörsi út 45, Budapest 1112, Hungary
- ³ Institute for Geological and Geochemical Research, Research Centre for Astronomy and Earth Sciences, Budaörsi út 45, Budapest 1112, Hungary
- ⁴ Mining and Geological Survey of Hungary, Columbus u. 17-23, Budapest 1145, Hungary

Introduction

Due to the growth of industrial activity and the continuous expansion of the technological infrastructure since the 19th century, the number of CO₂ emitting point sources and the amount of CO₂ gas releasing into the atmosphere have increased dramatically. The atmospheric proportion of CO₂ has now exceeded 410 ppm under continuous, large-scale emissions (NOAA/ESRL 2019). Carbon dioxide accumulating in the atmosphere is thought to pose a heavy environmental risk to the society today, as it plays a major role in global climate change as a greenhouse gas, thus affecting the ecosystem and water balance of the Earth (IPCC

2007). Therefore, reducing CO₂ emissions has a priority for the future of the Earth, which can only be achieved through extensive international cooperation (e.g.: Kyoto Protocol 1998; 2009/31/EC Directive 2009, Paris Agreement 2015).

A possible way to reduce emissions is separating the CO₂ from industrial flue gas and storing it in deep geological reservoirs (Carbon Capture and Storage—CCS) (Arts et al. 2008; IPCC 2013; De Silva et al. 2015). One of the most important pre-conditions for using this technology is to understand and predict the geochemical changes occurring during the storage process as accurately as possible. Several methods can help to understand the underground processes, such as laboratory experiments (e.g., Hellevang et al. 2010; De Silva et al. 2015), geochemical model-based approaches (e.g., Xu et al. 2003; Király 2017), and study of natural CO₂ accumulation areas or CO₂ analogues (e.g., Worden 2006; Király et al. 2016). It is important to study characteristic properties of the CO₂ natural analogues to understand what physical and chemical processes in an industrial CO₂ storage project are likely to occur. In other words, what are the necessary conditions for the long-term safety and efficiency of CO₂ trapping in deep geological environments (Watson et al. 2004). Mineral and petrophysical (porosity, permeability) properties of rocks are primarily determined by the conditions of their formation. This is especially true for sedimentary rocks where sedimentation and diagenetic processes primarily influence, among others, porosity, permeability, and reactivity. Therefore, it is essential that we know the environment and formation mechanism of rocks when examining CO₂ natural analogues (Pearce et al. 2005; Holloway et al. 2007).

Former studies have focused mainly on sandstone reservoirs, whereas conglomerate rocks have been neglected in terms of CO₂ storage due to their generally small volume and heterogeneity. However, the main objective of this study is to analyze the lithology and the geochemical character of conglomerate core samples that serve as natural CO₂ reservoirs in the Mihályi-Répcelak area, gaining a more accurate understanding of how lithology and pore water geochemistry influence CO₂ impacts in a natural environment.

This paper focuses on a distinctive isolated conglomerate reservoir at Mihályi-Répcelak area. Previous studies of conglomerate rocks, especially regarding CO₂ storage, are subordinate in the literature despite evidence suggesting natural CO₂ can accumulate in conglomerate reservoirs (Rauzi 1999). Nevertheless, conglomerate reservoirs could have a potential for CO₂ storage as based on our results, mineral trapping of CO₂ might also take place in the conglomerate rocks. Not considering mineral trapping, it was demonstrated by laboratory experiments (Wang et al. 2016) in Janggi basin (South Korea) that, due to favorable reservoir parameters, conglomerate rocks can store almost three times as much CO₂ as sandstones with similar porosity and depth.

Consequently, it also points to the importance of detailed or even targeted investigation of potential conglomerate reservoirs like the ones at the Mihályi-Répcelak area.

The present study investigates a well-known and extensively studied natural CO₂ accumulation at Mihályi-Répcelak area, north-western Hungary, where effects of CO₂ accumulation were examined in details for sandstone reservoirs and their caprocks (Király et al. 2016; Király 2017). A further study from the Mihályi-Répcelak area deals with the question of stable isotope composition of carbonate minerals, mainly dawsonite (Cseresznyés et al. 2017). The results show that dawsonite precipitated from magmatic CO₂, and the origin of OH is the pore water. One of the main questions of this study is whether the origin of dawsonite is the same in the conglomerate rock as in the sandstone.

Furthermore, accumulated CO₂ appearing in conglomerate rocks is exclusive and has not been studied before at Mihályi-Répcelak area nor worldwide, even though CO₂ trapping could be observed from new perspectives. The results from this study could be used to widen the knowledge about CO₂-rock-porewater systems and help to make industrial CO₂ geological storage safe and effective. Furthermore, conglomerates in the area represent a deeper stratigraphic unit than the sandstones, with remarkably different lithology and hypersaline pore water (Mészáros et al. 1979).

Geological background

Sedimentology and stratigraphy of the Little Hungarian Plain

Mihályi-Répcelak area is located in the Little Hungarian Plain, NW Hungary (Fig. 1), which is an extensional basin formed by NE–SW-striking faults during the Miocene and filled with Neogene sediments (Horváth 1993; Tari 1994; Kovač et al. 2007).

The pre-Pannonian sedimentary filling of Little Hungarian Plain is similar to other parts of the Pannonian Basin System. From Carpathian to Badenian, marine sediments of the Paratethys and coarse-grained alluvial sediments were formed (Sacchi and Horváth 2002; Kovač et al. 2007; Nagymarosy and Hámor 2012). The marine sediment sequences are interrupted by several tuff interbeddings which are connected to volcanic centers of Pásztori, Szany, and Tét area (Balázs and Nusszer 1987). Sarmatian sediments are represented by restricted brackish deposits of the Pannonian Lake. At the end of the Sarmatian, the Pannonian Lake lost all connection with oceans which caused gradual appearance of freshwater deposits and endemic fauna (Magyar et al. 1999).

Uplifting and erosion of Alpine-Carpathian region caused significant quantities of sediments transported to the

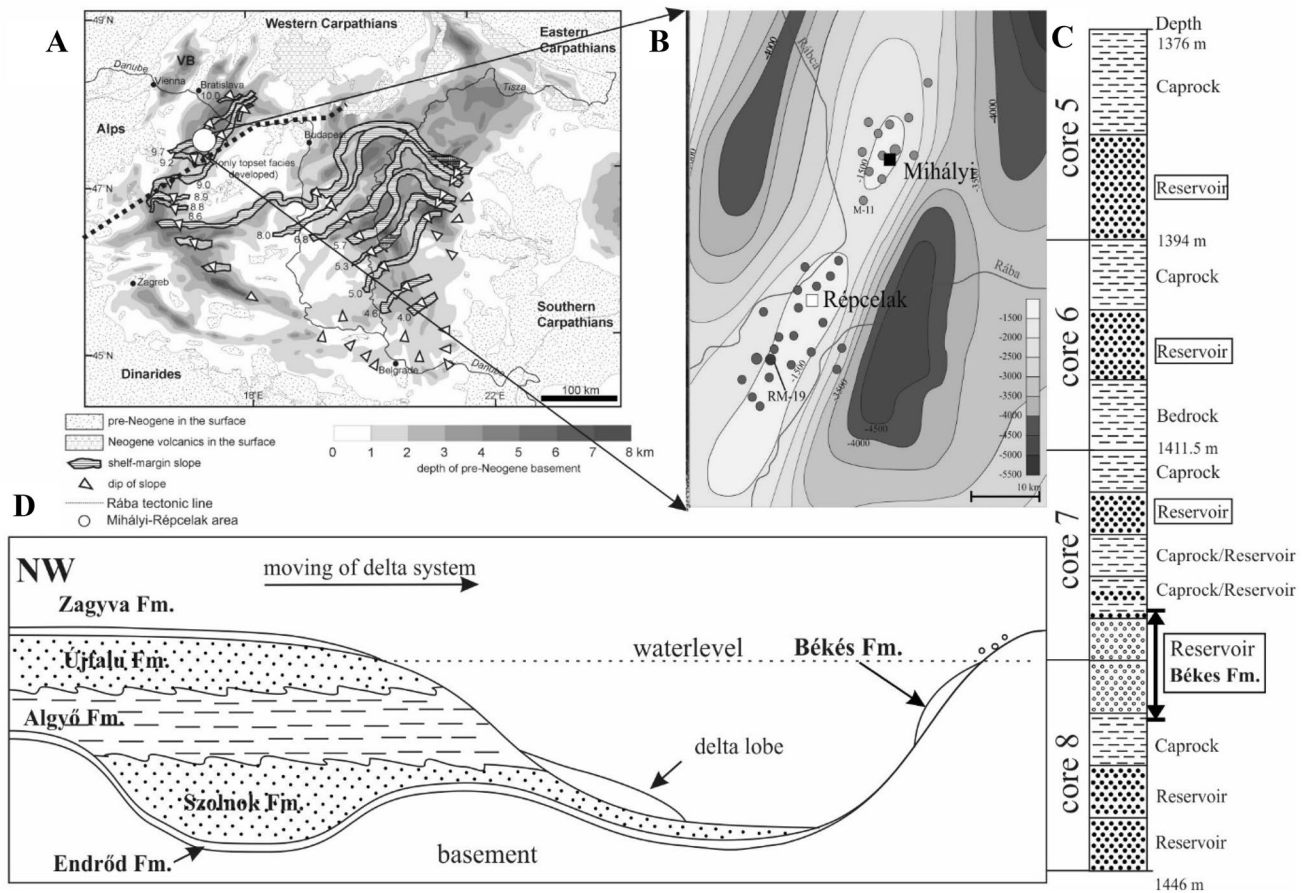


Fig. 1 Filling mechanism of the Pannonian Basin, where the Mihályi-Répcelak area signed with circle (modified after Magyar et al. 2013) (A). Topography map of the basement at Mihályi-Répcelak area (Zilahi-Sebess 2013) on which Mihályi- high is shown and black square marks the studied well (RM19) (B) schematic sequence of the

well contains several CO₂ reservoirs (square mark) (C). Theoretical filling model of the Little Hungarian Plain (based on Juhász 1998) shows studied rocks formed at the flank of islands as coarse erosional sediments during Lower Pannonian (D)

Pannonian Basin from the NW and started to fill the basin in the Late Miocene (Pogácsás 1984; Vakarcz et al. 1994; Juhász 1994, 1998; Magyar et al. 1999, 2013). The first shelf in the Little Hungarian Plain had formed 10 million years ago in less than 1 million years (Magyar et al. 2013). Starting from the Middle Miocene, the sedimentation was controlled by a prograding delta system arriving from the NW. The sediment sequence is uniform throughout the Pannonian Basin and reaches several km in thickness. This sequence hosts the most significant hydrocarbon, natural CO₂, and geothermal fluid resources basin wide.

The stratigraphically deeper units are characterized by alternating clayey-silty layers with fine-grained sand covered by a silt-dominated sequence. The shallower units are more dominated by medium-to-coarse grain size sand layers that are overlain by clayey layers, the latter representing fluvial sediments (Juhász 1994; Sztanó et al. 2013, 2016; Fig. 1C).

At some parts of the basin, the riffles of the basement reached the water level forming islands where abrasion sediments settled (Békés Formation) as assorted, unbedded conglomerates (Fig. 1C). Base material of these sediments is fine-grained sandstone with rounded gravels. It reaches its maximum thickness at the limb of structural highs, while it pinches out vertically (Juhász 1994). During recent research, Békés Formation was investigated by core samples, which are from 1411.5 to 1446.5 m depth. In every case, this formation is overlain by a dark gray to light gray, laminated to structureless clay marl serving as impermeable clayey cap rock.

Volcanic activity during the Neogene in the Little Hungarian Plain

In the Little Hungarian Plain, Late Miocene magmatic activity took place in two main phases. The Upper Miocene activity is represented by a buried magmatic body

characterized by a large positive magnetic anomaly in Pásztori area (Balázs and Nusszer 1987). Several oil exploration drills had reached the magmatic series and discovered a unique series of alkaline trachyte in the Pannonian Basin (Kőrössy 1958). The appearance of sea sediments at the beginning of the volcanic series suggests that volcanism began in a sub-sea environment (Kőrössy 1958; Harangi et al. 1995), but increased above sea level in the Sarmatian (Tari 1994). The second magmatic phase began 6 million years ago and volcanic cones built up by alkaline basalt, basanite, and trachybasalt formed in the Little Hungarian Plain area (Balázs and Nusszer 1987; Harangi et al. 1995).

Forming of CO₂ accumulation

As a result of volcanic activity, several CO₂ reservoirs developed in the area in the sandstone and conglomerate bodies of the Middle Miocene sedimentary sequence (Mészáros et al. 1979) (Fig. 1B). In the study area, 26 of these reservoirs have been exploited and produced in the last decades. The origin of the CO₂ was identified as magmatic (Palcsu et al. 2014; Vető et al. 2014) based on stable isotope composition of the produced gas.

Samples and methods

Samples

Two drill cores representing conglomerate facies (RM19-7Rkong and RM19-8Rkong), the only samples available from over 40 boreholes, were studied whose features are shown in Table 1. The drill cores available from the area predominantly consist of layered sandstones, aleurolites, and claystones.

Both studied samples are oligomictic, well cemented, matrix supported conglomerates. In both cases, the matrix is light gray-colored and fine-grained. The appearing clasts can be sorted in three groups, which are the following: (1) kaolinitic clasts that are 0.1–2.5 cm and make at least 50 v/v% of all clasts in the rocks, (2) mm-to-cm scale fossils, and (3) metamorphic and micrite rock fragments.

Petrography

During the sample preparation, two-component araldite resin was used with blue dye to make the porosity of the rock visible. The petrographic examination of the samples was carried out using an NIKON Eclipse LV100 POL type polarization microscope equipped with a NIKON DS-Fi1 digital. To get a better understanding of mineralogical and textural information, scanning electron microscopy (SEM) measurements were carried out. The Amray 1830-type electron microscopy was equipped with EDAX PV 9800 energy-dispersive X-ray spectrometer. 20 kV accelerating voltage was used in each case; the primary electron current was 1 nA. Backscattered electron (BSE) image and secondary electron image (SEI) were used during the analyses. Petrographic characterization and SEM analysis were carried out at the Eötvös Loránd University, Hungary.

Mineral modes were determined using X-ray Powder Diffraction (XRD) measurements. However, it must be noted, that several mineral phases identified under polarization microscope were not detectable during the XRD measurements. That is why, the mineral composition of the kaolinitic clasts (discussed in detail later) was estimated using image analysis on high-resolution SEM images. Volume of pores space (in v/v%) was taken by the difference between the total pixel number and the pixel number of all the minerals. After subtracting, the area filled with minerals from the size of the whole image. The error of this porosity calculation method can be up to 5–10 v/v% due to the granules lost during grinding.

Micro-XRD

Check the cleanness of the separated kaolinite samples to the stable isotope analysis, Micro-XRD were carried out at the Institute for Geological and Geochemical Research, Budapest. Micro-XRD analysis was performed following Kovács et al. (2021) on an RIGAKU D/MAX RAPID II diffractometer, which is a combination of a MicroMax-003 third-generation microfocussing, sealed-tube X-ray generator, and a curved imaging plate (IP) detector. The diffractometer is operated with CuK α radiation generated at 50 kV and 0.6 mA. The powdered samples for the micro-diffraction measurements

Table 1 Studied samples properties

Samples	Depth (m)	Temperature (°C)	Kaolinitic clasts [v/v %]	Fossils [v/v %]	Other clasts [v/v %]	Organic material [v/v %]	Weight [g]
RM19-7Rkong	1411.5–1429	68.16	~50	~40	~5	~5	594.54
RM19-8Rkong	1429–1446	68.84	~65	~25	~10	–	505.06

The temperature was estimated by average geothermal gradient (Dövényi et al. 1983) and the average mean temperature at the area (Hungarian Meteorological Service 2018)

are encapsulated in a borosilicate-glass capillary, with a diameter of 0.3 mm and wall thickness of 0.01 mm, by a vertical manual charging process. Then, the capillary is analyzed by the micro-diffractometer in transmission mode with a beam spot diameter of 100 μm . In each measurement, 0.5–1 mg sample is placed in the funnel end of the capillary and the sample is tapped into the narrow portion. The measurement time takes about 10 min. IP is read by a laser scanning readout system in about 1 min. 2DP RIGAKU software is used to record the diffraction image from the laser readout and the operator can determine the area to integrate for a 2 θ versus intensity plot. This plot is read into RIGAKU PDXL 1.8 software for data interpretation. The diffraction patterns were processed using SiroQuant V4 software, and the modal contents were determined by the Rietveld method.

Stable isotope measurements

Water contents and H isotope compositions were determined using a High-Temperature Conversion Elemental Analyser (TC/EA) attached to a stable isotope ratio measuring mass spectrometer (Sharp et al., 2001) at the Institute for Geological and Geochemical Research, Budapest. Kaolinite samples were wrapped into Ag foil capsules, placed into a heatable carousel (Uni-prepTM, Eurovector SpA, Italy), heated to 100 °C while pumped for an hour using a Cole Palmer[®] Air Cadet[®] diaphragm pump and a liquid nitrogen trap. The samples were then flushed with He and dropped into the high-temperature conversion unit (TC/EA) in a continuous flux of He carrier gas. The reaction tube was packed with glassy carbon and heated to 1430 °C. At the reaction temperature, H-bearing minerals release their volatile content and the evolving H₂O is converted to H₂ gas. The TC/EA unit was attached to a Thermo Finnigan delta V mass spectrometer, which was used to determine D/H ratios in the H₂ gas. The hydrogen contents were calculated on the base of size of the mass 2 signal peak. The isotope compositions were expressed in the δ -notation ($\delta^2\text{H}=(R_1/R_2-1)\cdot 1000$, where R_1 and R_2 are the D/H ratios in the sample and the standard, respectively) in permil (‰) relative to V-SMOW. The H isotope compositions of laboratory standards (IAEA CH-7 polyethylene foil and NBS-22 oil) were used for calibration yielded an average reproducibility of $<\pm 2$ ‰. A $\delta^2\text{H}$ value of -27.5 ± 0.7 ‰ ($n = 4$) was obtained for an in-house test amphibole sample (TOB-A1) that had been analyzed before at the University of Lausanne (-29 ‰, Demény et al., 2005) and at the Université Claude Bernard Lyon 1 (-28.6 ± 6.0 ‰, $n = 5$; Fourel et al. 2017). Note that the He flushing method without heating resulted in a $\delta^2\text{H}$ value of -28.8 ± 4.8 ‰ ($n = 4$), closer to the published values. The NBS-30 biotite standard was measured, but yielded a large scatter (from -64 to -56 ‰) in accordance with the observations of Qi et al. (2014).

Calculation of δD values in pore water in equilibrium with kaolinite

The calculations were based on results of δD measurements in kaolinite and published fractionation equations (Faure 1998; Savin and Epstein 1970; Suzuoki and Epstein 1976; Lambert and Epstein 1980). Formation temperature ($T = 70$ °C) was estimated from the current depth (1411.5–1446 m) of the studied samples, the average geothermal gradient at the Little Hungarian Plain area (40 °C/km) (Dövényi et al. 1983) and the average mean temperature of the area (11 °C) (Hungarian Meteorological Service 2018).

Savin and Epstein (1970) and Suzuoki and Epstein (1976) suggested constant kaolinite–water hydrogen-isotope fractionation values of -30 ‰ and -23.4 ‰, respectively. On the other hand, Lambert and Epstein (1980) found temperature dependence in the fractionation and gave the following equation: $1000\cdot\ln\alpha = -4.53\cdot 106/T^2 + 19.4$. Assuming 70 °C as formation temperature (see above), the hydrogen-isotope fractionation value is -19.1 ‰. Since $\alpha = (\delta\text{D}_{\text{kaolinite}} + 1000)/(\delta\text{D}_{\text{water}} + 1000)$, the water composition can be calculated using the measured kaolinite compositions. To reduce the uncertainties inherent in the fractionation values given by the studies listed above, all of the calculated water compositions are reported and finally averaged.

Results

Petrography of the conglomerates

The base material consists of moderately abrasive monocrystalline quartz, mica, and plagioclase. They appear as detrital minerals. Accessory apatite, glauconite, Ti-containing minerals (rutile or anatase), pyrite, and zircon were also found. In some cases, diagenetic quartz growth was observed on the detrital quartz particles. Mica appears unoriented and shows no signs of deformation or dissolution. The plagioclase particles of size 300–450 μm occur in minimal quantities (one or two grains) in both samples. The cement material of the rocks is carbonate based on scanning electron microscopic measurements and mainly consists of calcite. In addition, minimal amounts of siderite and ankerite appear.

Fossils in the conglomerates

In the samples, 25–40 v/v% of all clasts are fossils ranging in size from 100 to 2 mm, and in all cases, they are built up by calcite. Fossils in the samples can be classified into two groups. In the matrix Ostracoda, Gastropoda, and various shells and shell fragments are dominant. Additionally, dark brown, rounded micrite fragments *Milionida* sp., *Elphidium* sp., and *Sprulina* sp. foraminifera were found (Galácz and Monostori 1992).

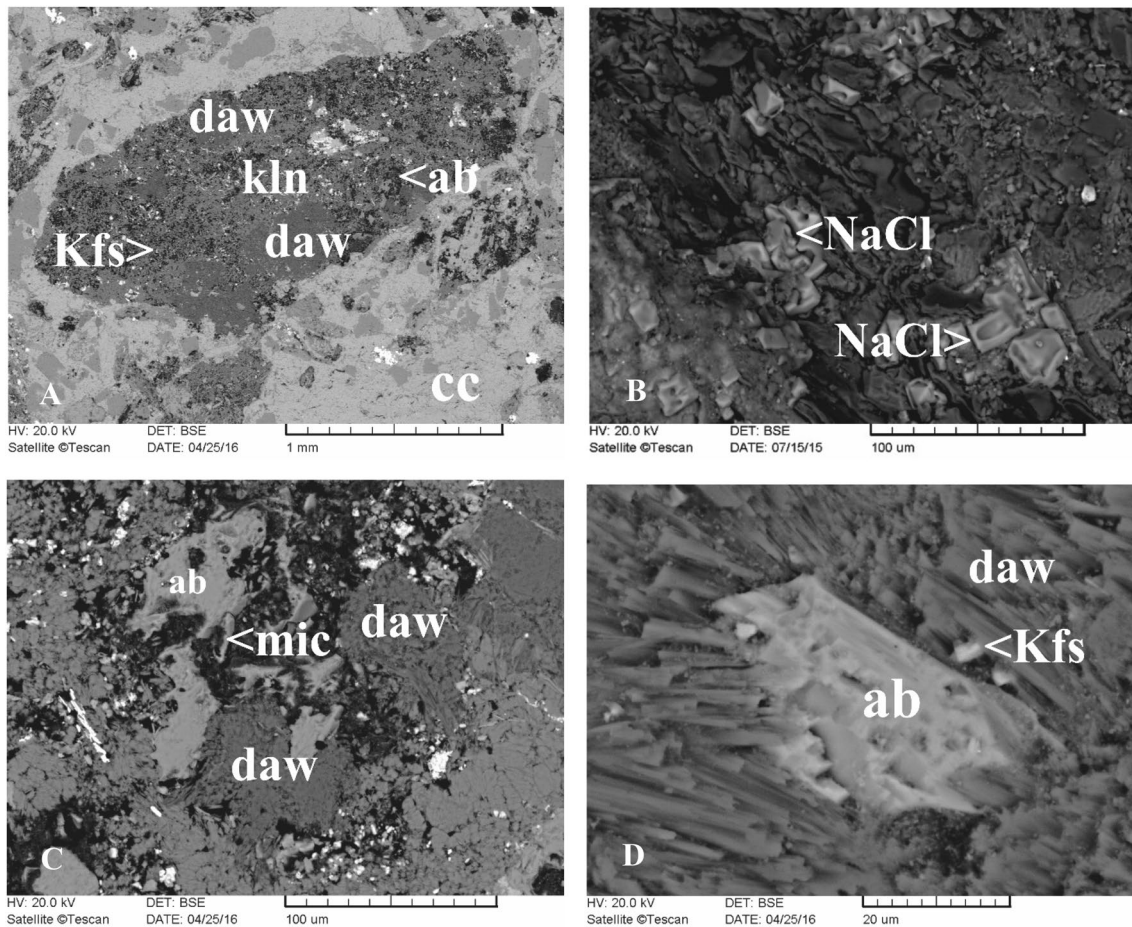


Fig. 2 Dawsonite appears at the rim of kaolinitic clasts (**A**, SEM BSE) in which halite also appears (**B**, SEM BSE) as an evidence of salt-saturated pore water. In the direct surrounding of dawsonite, relict albite

can be detached (**C**; SEM BSE) just like between dawsonite fibers (**D**; SEM BSE). *daw* dawsonite, *kln* kaolinite, *mic* mica, *Kfs* K-feldspar, *ab* albite, *cc* calcite, *NaCl* halite

Table 2 Modal composition based on image analysis of the kaolinitic clasts

	RM19-7Rkong v/v%	RM19-8Rkong v/v%
Kaolinite	60	54
Mica	6	13
Dawsonite	5	7
K-feldspar	4	4
Pyrite + TiO ²	2	6
Ankerite + siderite	2	5
Albite	1	7
Calcite	tr	tr
Halite	tr	tr
SiO ²	tr	tr
Pore	20	13

Minerals with gray background are diagenetic, while white ones are detrital. Tr is less than 1 v/v%

Petrography of kaolinitic clasts in the conglomerates

Kaolinitic clasts in the studied conglomerates are rounded (Fig. 2A). Results of staining method used in sample preparation implies that porosity in kaolinitic clasts is considerably higher (according to visibility of the blue epoxy) than in the matrix where the used blue dye can be detected only on micrometer scale.

According to the SEM analysis, the main mineral in the kaolinitic clasts is kaolinite (~53–70 v/v %) (Table 2). Kaolinite appears only in the kaolinitic clasts (Fig. 2A). The clasts display relict magmatic textures most likely representing intersertal structure with mica, albite, K-feldspar, Ti-minerals (rutile or anatase) apatite, and opaque minerals occurring in the clasts. These phases are considered to be part of the original material. Halite (Fig. 2B), dawsonite, and other carbonate minerals appear as diagenetic minerals. Dawsonite, a new mineral phase in the rocks is the strongest evidence of CO₂ presence (Worden 2006), is limited to the rim of kaolinitic

clasts. The dawsonites in the kaolinitic clasts appear as radial, fibrous minerals. The fibers reach over the edge of the kaolinitic clasts (Fig. 2A), which indicates that dawsonite is a diagenetic mineral. Between the fibers of dawsonite, relict albite and K-feldspar are observed (Fig. 2C and D).

Modal composition of the kaolinitic clasts in the two samples is similar to each other except in the presence of halite (Fig. 2B) which can be identified only in RM19-7Rkong sample. However, mineral modes strongly differ in the samples. Quantity of albite decreases with the occurrence of dawsonite in the two samples. In the RM19-7Rkong sample, there is 3 v/v% surplus in dawsonite, while it has 6 v/v% less albite than in RM19-8Rkong sample (Table 2). Pore space in the RM19-8Rkong sample is lower than in RM19-7Rkong (RM19-7Rkong: 20.36 v/v%; RM19-8Rkong: 13.36 v/v%).

Micro-XRD

According to the micro-XRD analyses, the separated kaolinite samples are clean (57–76 m/m%). Further minerals are quartz (6–20 m/m%), feldspar (3–15 m/m%), calcite (5–9 m/m%), and alunite (3–6 m/m%). Two samples contained mica (3 and 7 m/m%, Table 3).

Table 3 δD values from kaolinitic clasts

Sample	Sampling method	Dawsonite	δD [‰]
RM19-7Rkong	Micro-sampling	+	− 63.0
RM19-7Rkong	Micro-sampling	+	− 55.5
RM19-7Rkong	Micro-sampling	+	− 56.9
RM19-7Rkong	Homogenized	−	− 56.6
RM19-7Rkong	Homogenized	−	− 57.3
RM19-8Rkong	Homogenized	−	− 55.9
RM19-8Rkong	Homogenized	−	− 55.4

In the table, ‘+’ means the sampling was carried out in dawsonite-bearing kaolinitic clasts. ‘−’ means the homogenized samples are from dawsonite-free clasts. The gray-colored samples contained mica (3 and 7 m/m %)

Table 4 Calculated δD values in pore water in equilibrium with kaolinite at the estimated formation temperature ($T=70$ °C)

Sample	Dawsonite	δD_{water} [‰]		
		Savin and Epstein (1970)	Suzuoki and Epstein (1976)	Lambert and Epstein (1980)
RM19-7Rkong	+	− 34.5	− 40.8	− 45.0
RM19-7Rkong	+	− 26.7	− 33.1	− 37.3
RM19-7Rkong	+	− 28.2	− 34.6	− 38.7
RM19-7Rkong	−	− 27.9	− 34.3	− 38.4
RM19-7Rkong	−	− 28.6	− 35.0	− 39.2
RM19-8Rkong	−	− 27.1	− 33.5	− 37.7
RM19-8Rkong	−	− 26.6	− 33.0	− 37.2
Average δD_{water} [‰]	− 34.2 ‰			

Calculations were based on different empirical fractionation factors from the literature

Stable isotope measurements in kaolinitic clasts

The relatively high hydroxyl content (OH^-) of kaolinite allowed δD values to be measured in the kaolinitic clasts. Two types of samplings were carried out: (1) homogenized samples from kaolinitic clasts that are dawsonite barren and (2) controlled micro-sampling from preselected areas in the kaolinitic clasts near dawsonite precipitation. The results show that the samples containing dawsonite show slightly different δD values than the ones without dawsonite. The differences may depend on the quantity of dawsonite in the micro-sampling. The presence of dawsonite may cause a decrease in δD values. Results are shown in Table 3.

In dawsonite-bearing kaolinitic clasts, δD values are between − 63.0 ‰ and − 55.5 ‰, whereas in the RM19-8Rkong, the δD values are − 55.4 ‰ and − 55.9 ‰ (Table 3). Table 4 summarizes the calculated δD values in pore water considering three different kaolinite water fractionation values, whereas the average δD_{water} values in dawsonite-bearing and dawsonite-free samples are shown in Table 5.

Discussion

Depositional environment

Based on the foraminiferas, *Miliolina* sp., *Elphidium* sp., *Spirulina* sp. in the micrite rock fragments, represent

Table 5 Average calculated δD values in pore water in equilibrium with kaolinite separated the dawsonite-bearing clasts from dawsonite-free clasts

	δD_{water} [‰]
Dawsonite-bearing clasts	− 35.4
Dawsonite-free clasts	− 33.2

euhaline water of Badenian- Sarmatian (15.9–11.6 Ma) (Galácz and Monostori 1992). However, fossils, Ostracoda, Gastropoda, and shell fragments, in the matrix refer to brackish water environment (Galácz and Monostori 1992). This means redeposition that involved the studied conglomerates happened in the Pannonian time and affected the Badenian–Sarmatian sediments. In both studied samples, the appearing clasts are elongated and show a slight orientation. This may refer to episodic events, like storms, mass movements, or changing weather conditions, which caused the redeposition and formation of the conglomerates from Badenian–Sarmatian and Pannonian sediments.

The kaolinitic clasts, based on our petrographic observations, represent altered volcanoclastic fragments that have experienced transport resulting in rounded shapes. It is a question whether kaolinitization of the clasts precedes transport and sedimentation or is already the manifestation of diagenetic alteration.

The preservation of original volcanic intersertal texture strongly implies that the alteration process took place after transport and sedimentation. The relics of mica and feldspars, partly kaolinitized and the lack of quartz indicate that

the original rocks, from which the kaolinitic clasts formed, were probably neutral pyroclasts. These rocks could be related to the Pásztori volcano, which were active during the same time period as the formation of studied rocks (~ 10 million year ago; Harangi et al. 1995) and marked as a possible source of CO₂ migration (Vető et al. 2014). The dominant textural type, identified in the rocks derived from the volcanism from Pásztori volcano, is also intersertal (Schléder 2001), which also supports the connection between the studied rocks and Pásztori volcano. However, we cannot completely rule out the possibility that the former volcanic clast was transported already as kaolinite.

Dawsonite formation environment

After the deposition and burial of the sediments, diagenetic effects caused remarkable changes on the properties of rocks, especially in mineral composition including the formation of dawsonite. Its appearance as a new mineral is a result of CO₂–pore water–host rock interaction.

Dawsonite fibers cross the border between the kaolinitic clast and the base material, which indicates that dawsonite

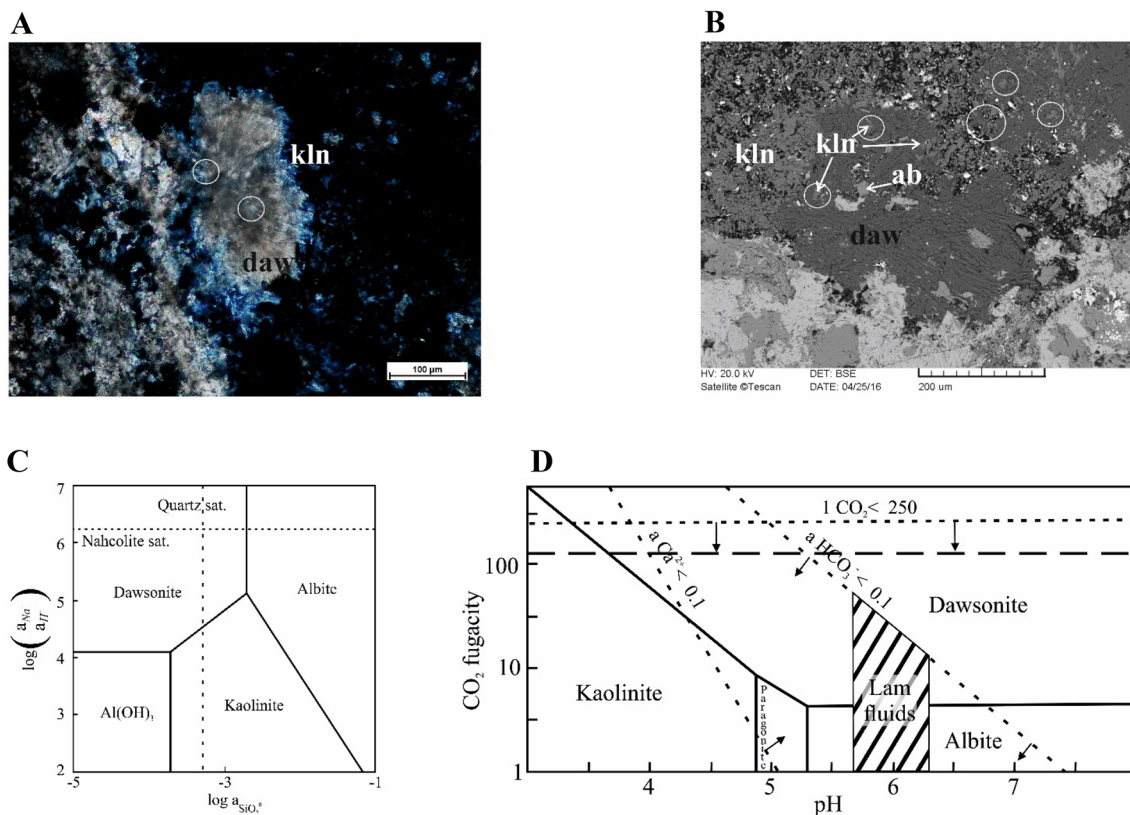


Fig. 3 Dawsonite stability at the studied environment. Dawsonite precipitated in the edge of kaolinitic clast (XN, polarization microscope) (A), Albite relict occurred in the environment of dawsonite, which mixed with kaolinite (white circles) (B). CO₂ fugacity–pH diagram

(Worden 2006), where the dashed line signed the actual CO₂ fugacity (C). Dawsonite stability depends on Na⁺ concentration, pH, and SiO₂ activity (Hellevang et al. 2013) (D)

appears as diagenetic mineral; hence, it was formed after the burial. Feldspar relicts—mostly albite and K-feldspar—between fibers of dawsonite refer to the breakdown of albite and K-feldspar to form dawsonite (Fig. 3A). This observed process corresponds to models (Worden 2006; Zhou et al. 2014) that state the Al^{3+} content of dawsonite comes from dissolution of albite and K-feldspars; meanwhile, the source of Na^+ content of dawsonite could be either the dissolved albite and/or, if K-feldspar was the source of Al^{3+} , Na^+ may have originated from the pore water itself. The presence of considerable concentrations of Na^+ in pore water is also supported by halite in RM19-7Rkong sample (Table 2), which refers the pore water being (over)saturated in NaCl.

We suggest that the strongly limited nature of dawsonite forming processes in the conglomerates, compared to overlying sandstones (Király et al. 2016), can be related to the high salinity and, therefore, low CO_2 solubility in the system. The appearance of halite confirms the high salinity in the pore water. In a $\text{NaCl-H}_2\text{O-CO}_2$ system, CO_2 activity dramatically decreases as the salt content grows (e.g., Duan et al., 2006). Therefore, the presence of CO_2 is mostly expected as free phase, resulting in much lower reactivity compared to dissolved CO_2 and lower degree of pore water–reservoir rock interaction. However, it is notable that the formation of dawsonite vs. kaolinite depends strongly on the geochemical environment. Furthermore, we should consider the microenvironment of the observed mineral reactions. Kaolinite and dawsonite are intergrown around the rims of kaolinitic clasts in close textural relation with (Fig. 3A,B), albite and K-feldspar relicts (Figs. 2D, 3B). This may indicate that a microenvironment favorable for dawsonite formation could have developed only at the rims of the kaolinitic clasts on the kaolinite-dawsonite equilibrium (Fig. 3A, B).

In this geochemical system, besides CO_2 fugacity (Worden 2006, Fig. 3C), the formation of kaolinite or dawsonite depends on the pH, Na^+ concentration, and SiO_2 activity (Hellevang et al. 2013, Fig. 3D). The conditions for dawsonite formation were only appropriate at the rim of the kaolinitic clasts where silicate minerals could dissolve, whereas Na^+ and Al^{3+} were supplied and CO_2 fugacity was adequately high for the stability of dawsonite. The exclusive occurrence of dawsonite on clast rims might be related to sudden increase in porosity from the matrix to kaolinitic clasts and the resulting in abrupt changes in the dynamics of the pore water flow. Thus, the controlled appearance of dawsonite is a combined effect of several phenomena. It is interesting that physical and geochemical conditions for the formation of dawsonite should have been appropriate in the whole kaolinitic clast; however, dawsonite formed only at the clast rims (Figs. 2A, 3A).

Possible origin of the dawsonite-bearing kaolinite forming pore water

Considering that the rock is not composed of significant amount of hydrogen-bearing minerals (minerals with crystalline water or OH^- content), which would influence the δD values of the percolating water, the hydrogen-isotope composition of kaolinite represents the percolating water during the formation of kaolinite. Based on the rounded shape of kaolinitic clasts (Fig. 2A), the alteration of sediments into kaolinite clasts may have started during early lithification, which means the present pore water may have come from the infiltrating meteoric water. Since the dawsonite-bearing kaolinite clasts yield almost the same water hydrogen isotope composition (-35.4‰) as the dawsonite-free clasts do (-33.2‰) (see Table 5), the isotopic compositions of the percolating solutions may have been similar during kaolinite and dawsonite formation (related to fluid origin), regardless the chemical differences that might have been determined by water-rock interactions

However, the average calculated $\delta\text{D}_{\text{water}}$ value (-34.2‰) does not match the composition of present day meteoric water in Hungary (annual mean of -62.3‰ , Czuppon et al. 2018), but has slightly higher values. More likely, the calculated $\delta\text{D}_{\text{water}}$ values reflect climatic condition of Late Miocene/Pliocene, which had largely homogenous, warm, and humid climate (Burch et al. 2006; Kovács et al. 2015), and caused a higher δD value in meteoric water (Fig. 4).

Considering the origin of pore water, the increased local geothermal heat flow, as results of volcanic activity in the area during Upper Miocene, caused emergence of convection flow in groundwater system. Mixing of magmatic water to the infiltrating solutions along with the CO_2 cannot be excluded, but, in this case, the meteoric water should have had even higher H isotope compositions than magmatic water, which has generally lower δD values (around -80‰ , Boettcher and O'Neil 1980; Kyser and O'Neil 1984).

Concluding remarks

The present study investigated effects of natural CO_2 flooding on a conglomerate formation at Mihályi-Répcelak area in Hungary. The studied conglomerate rocks formed by episodic redeposition during the Lower Pannonian era (~10 million years ago) and became CO_2 reservoirs in the same era.

The presence of dawsonite is the clearest evidence of CO_2 interaction, which means that at least part of the CO_2 trapped in mineral form. The variability in porosity and mineral composition within the studied conglomerates strongly

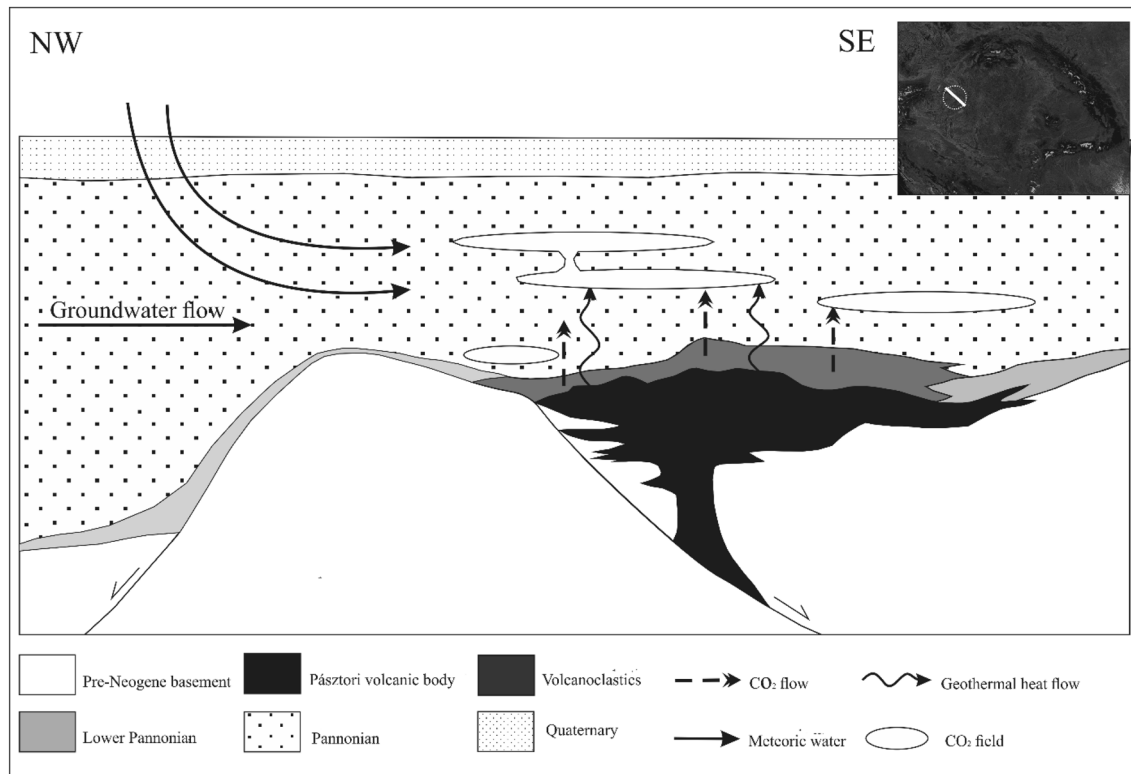


Fig. 4 Schematic figure about processes at the area (based on Panisova et al. 2017). Accumulated CO₂ at the area connected to volcanism along the Rába line (Pásztori volcano). Accumulation fields interact with surrounding water

influences the reaction processes induced by the presence of CO₂. Beside the rock properties, the geological setting of the studied formation, facies, properties of surrounding rocks, and regional groundwater flow system also influence the CO₂-related processes.

Our results highlight the prevailing influence of geological setting of reservoirs such as relief of basement, the sedimentary sequence and the hydrogeological properties of the area, thereby the salinity of the system, which dramatically reduces the potential of mineral trapping of CO₂. Therefore, in case of a possible industrial CO₂ storage project, investigation of the mineral composition and caprocks alone is not sufficient. Significant attention should be given to the complete geological environment of the selected area. Otherwise, efficiency of CO₂ trapping during storage could be compromised, increasing the risk of any industrial CO₂ storage project.

Acknowledgements The study was carried out in cooperation between Eötvös Loránd University (ELTE) and Mining and Geological Survey of Hungary (MBFSZ) (contract numbers: TTK 2461/1/2013 and MBFSZ 206-114 / 2013) and was furthermore supported by the OTKA program (K-131353) of the National Research, Development and Innovation Office of Hungary, the ELTE Institutional Excellence Program (1783-3/2018/FEKUTSRAT) of the Hungarian Ministry of Human Capacities and ELTE Research and Instrument Core Facility (KKMC) (KMOP project number 4.2.1/B-10-2010-002). The Hungarian Academy of Sciences financially supported the stable isotope laboratory of the Institute

for Geological and Geochemical Research (Budapest) in the course of the study (INFRA-2018/310). We are grateful to Dan Uehara to correct our English in the article. Prepared with the professional support of the Doctoral Student Scholarship Program of the Co-operative Doctoral Program of the Ministry of Innovation and Technology Financed from the National Research, Development and Innovation Fund (KDP-2020-971244 to Dóra Cseresznyés).

Funding Open access funding provided by ELKH Research Centre for Astronomy and Earth Sciences.

Open Access This article is licensed under a Creative Commons Attribution 4.0 International License, which permits use, sharing, adaptation, distribution and reproduction in any medium or format, as long as you give appropriate credit to the original author(s) and the source, provide a link to the Creative Commons licence, and indicate if changes were made. The images or other third party material in this article are included in the article's Creative Commons licence, unless indicated otherwise in a credit line to the material. If material is not included in the article's Creative Commons licence and your intended use is not permitted by statutory regulation or exceeds the permitted use, you will need to obtain permission directly from the copyright holder. To view a copy of this licence, visit <http://creativecommons.org/licenses/by/4.0/>.

References

Arts R, Beaubien S, Benedictus T, Czernichowski-Lauriol I, Fabriol H, Gastine M, Gundogan O, Kirby G, Lombardi S, May F, Pearce J,

- Persoglia S, Rimmels G, Riley N, Sohrabi M, Stead R, Vercelli S, Vizika-Kavvadias O (2008) What does CO₂ geological storage really mean? CO₂ GeoNet Eur Netw Excell 20:20
- Balázs E, Nusszer A (1987) Magyarország medenceterületeinek kunsági (pannoniai s str) emeletbeli vulkanizmusa. In: LXIX. Yearbook of Geology Institute of Hungary. Budapest, Hungary, pp 95–103
- Boettcher AL, O'Neil JR (1980) Stable isotope, chemical and petrographic studies of high-pressure amphiboles and micas: Evidence for metasomatism in the mantle source regions of alkali basalts and kimberlites. *Am J Sci* 280:594–621
- Burch AA, Utescher T, Mosbrugger V, Gabrielyan I, Ivanov DA (2006) Late Miocene climate in the circum- Alpine realm: a quantitative analysis of terrestrial palaeofloras. *Peleogeography, Paleoclimatology, Paleocology* 238:270–280. <https://doi.org/10.1016/j.palaeo.2006.03.028>
- Cseresznyés D, Gy C, Zs S, Cs K, Cs S, Gy F (2017) Stable isotope compositions of different mineral phases found in a natural CO₂-reservoir (NW-Hungary): implication for their origin. *Energy Proced* 114:2812–2818. <https://doi.org/10.1016/j.egypro.2017.03.1399>
- Czuppon G, Demény A, Leél-Őssy S, Óvari M, Molnár M, Stieber J, Kiss K, Kármán K, Surányi G, Haszpra L (2018) Cave monitoring in the Béke and Baradla caves (Northeastern Hungary): implications for the conditions for the formation cave carbonates. *Int J Speleol* 47:13–28. <https://doi.org/10.5038/1827-806X.47.1.2110>
- De Silva GPD, Ranjith PG, Perera MSA (2015) Geochemical aspects of CO₂ sequestration in deep saline aquifers: a review. *Fuel* 155:128–143. <https://doi.org/10.1016/j.fuel.2015.03.045>
- Demény A, Vennemann TW, Homonnay Z, Milton A, Embey-Isztin A, Nagy G (2005) Origin of amphibole megacrysts in the Pliocene Pleistocene basalts of the Carpathian-Pannonian Region. *Geol Carpath* 56:179–189
- Dövényi P, Horváth F, Liebe P, Gálfi J, Erki J (1983) Geothermal conditions of Hungary. *Geophy Trans* 29:3–114
- Duan Z, Sun R, Zhu C, Chou IM (2006) An improved model for the calculation of CO₂ solubility in aqueous solutions containing Na⁺, K⁺, Ca²⁺, Mg²⁺, Cl⁻, and SO₄²⁻. *Mar Chem* 98:131–139. <https://doi.org/10.1016/j.marchem.2005.09.001>
- 2009/31/EK: Directive 2009/31/EC of the European Parliament and of the Council on the geological storage of carbon dioxide and amending Council Directive 85/337/EEC, European Parliament and Council Directives 2000/60/EC, 2001/80/EC, 2004/35/EC, 2006/12/EC, 2008/1/EC and Regulation (EC) No 1013/2006 (2009). <http://eur-lex.europa.eu/LexUriServ/LexUriServ.do?uri=OJ.L:2009:140:0114:0135:EN:PDF>. Accessed 23 Apr 2009
- Faure G (1998) Principles and applications of geochemistry. John Wiley and Sons Ltd, New Jersey, p 615
- Fourel F, Lécuyer C, Demény A, Boulvais P, Lange L, Jacob DE, Kovács I (2017) 2H/1H measurements of amphiboles and nominally anhydrous minerals (clinopyroxene, garnet and diamond) using high-temperature continuous flow elemental analyser/pyrolysis/isotope ratio mass spectrometry. *Rapid Commun Mass Spectrom* 31:2066–2072
- Galács A, Monostori M (1992) Paleontological Practicum. Tankönyvkiadó, Budapest, ISBN: 9631835634, p 663 (In Hungarian)
- Harangi S, Vaselli O, Tonarini S, Cs S, Harangi R, Coradossi N (1995) Petrogenesis of Neogene extension-related alkaline volcanic rocks of the Little Hungarian Plain Volcanic Field (Western Hungary). *Acta Vulcanol* 7(2):173–187
- Hellevang H, Aagaard P, Jahren J (2013) Will Dawsonite forming during CO₂ storage? *Greenhouse Gases Science and Technology* 4(2):191–199. <https://doi.org/10.1002/ghg.1378>
- Hellevang H, Declercq J, Kvamme B, Aagaard P (2010) The dissolution rates of dawsonite at pH 0.9 to 5 and temperature of 22, 60 and 77 °C. *Appl Geochem* 25(10):1575–1586. <https://doi.org/10.1016/j.apgeochem.2010.08.007>
- Holloway S, Pearce JM, Hards VL, Ohsumi T, Gale J (2007) Natural emissions of CO₂ from the geosphere and their bearing on the geological storage of carbon dioxide. *Energy* 32:1194–1201. <https://doi.org/10.1016/j.energy.2006.09.001>
- Horváth F (1993) Towards a mechanical model for information of the Pannonian basin. *Tectophysics* 226:333–357. [https://doi.org/10.1016/0040-1951\(93\)90126-5](https://doi.org/10.1016/0040-1951(93)90126-5)
- Hungarian Meteorological Service (2018) Magyarország éghajlata. https://www.met.hu/eghajlat/magyarorszag_eghajlata/eghajlati_visszatekinto/elmult_evek_idojarasa/main.php?ful=homerseklet. Accessed 10 Dec 2019
- IPCC (Intergovernmental Panel on Climate Change) (2007) Summary for policymakers. In: Solomon S, Qin D, Manning M, Chen Z, Marquis M, Averyt KB, Tignor M, Miller HL (eds) *Climate change 2007. The physical science basis. Contribution of working group I to the fourth assessment report of the intergovernmental panel on climate change*. Cambridge University Press, Cambridge, p 248
- IPCC (Intergovernmental Panel on Climate Change) (2013) Summary for policymakers. In: Stocker TF, Qin D, Plattner G-K, Tignor M, Allen SK, Boschung J, Nauels A, Xia Y, Bex V, Midgley PM (eds) *Climate change 2013: the physical science basis. contribution of working group I to the fifth assessment report of the intergovernmental panel on climate change*. Cambridge University Press, Cambridge
- Juhász G (1994) Magyarországi neogén medencérezek pannóniai s.l. üledéksorának összehasonlító elemzése. *Földtani Közöny* 124(4):341–365
- Juhász G (1998) A magyarországi neogén mélymedencék pannóniai képződményeinek litosztratiográfiája. In: Bérczi I, Jámor Á (eds) *Magyarország geológiai képződményeinek rétegtana. Magyar Olajipari Részvénytársaság és a Magyar Állami Földtani Intézet kiadása, Budapest, pp 469–484 (in Hungarian)*
- Király C (2017) Mihályi-Répcelak természetes CO₂-előfordulás környezetgeokémiai vizsgálata. PhD thesis, Eötvös Loránd University, Budapest, Hungary, p 161
- Király C, Sendula E, Szamosfalvi Á, Káldos R, Kónya P, Kovács II, Fűri J, Zs B, Gy F (2016) The relevance of dawsonite precipitation in CO₂ sequestration in the Mihályi-Répcelak area, NW Hungary. In: Armitage PJ, Butcher AR, Churchill JM, Csoma AE, Hollis C, Lander RH, Omma JE, Worden RH (eds) *Reservoir quality of clastic and carbonate rocks: analysis. Modelling and prediction geological society. London Special Publications, London, p 435*
- Kőrössi L (1958) Adatok a kisalföld mélyföldtanához. *Földtani Közöny* 88:291–298
- Kovač M, Andreyeva-Grigorovich A, Bajraktarevic Z, Brzobohaty R, Filipescu S, Fodor L, Harzhauser M, Nagymarosy A, Oszczypko N, Pavelic D, Rögl F, Saftic B, Slive L, Studencka B (2007) Badenian evolution of the Central Paratethys Sea: paleogeography, climate and eustatic sea-level changes. *Geol Carpath* 58(6):579–606
- Kovács J, Szabó P, Kocsis L, Vennemann T, Sabol M, Gasparik M, Virág A (2015) Pliocene and early pleistocene paleoenvironmental conditions in the Pannonian Basin (Hungary, Slovakia): stable isotope analyses of fossil proboscidean and perissodactyl teeth. *Peleogeography, Paleoclimatology, Paleocology* 440:455–466. <https://doi.org/10.1016/j.palaeo.2015.09.019>
- Kovács I, Németh T, KissBenkő BGZ (2021) Application of capillary method in micro X-ray diffractometry (μ-XRD): a useful technique for the characterisation of small amounts of clay minerals. *Cent Eur Geol*. <https://doi.org/10.1556/24.2020.00005>
- Kyoto Protocol (1998) Kyoto protocol to the United Nations framework convention on climate change. <https://unfccc.int/resource/docs/convkp/kpeng.pdf>
- Kyser TK, O'Neil JR (1984) Hydrogen isotope systematics of submarine basalts. *Geochim Cosmochim Acta* 48:2123–2133

- Lambert SJ, Epstein S (1980) Stable isotope investigations of an active geothermal system in Valles Caldera, Jemez Mountains, New Mexico. *J Volcanol Geoth Res* 8:111–129
- Magyar I, Geary HD, Müller P (1999) Paleogeographic evolution of the Late Miocene Lake Pannon in Central Europe. *Palaeogeogr Palaeoclimatol Palaeoecol* 147:151–167. [https://doi.org/10.1016/S0031-0182\(98\)00155-2](https://doi.org/10.1016/S0031-0182(98)00155-2)
- Magyar I, Radivojević D, Sztanó O, Synak R, Ujvási K, Pócsik M (2013) Progradation of the paleo Danube shelf margin across the Pannonian Basin during the Late Miocene and Early Pliocene. *Global Planet Change* 103:168–173. <https://doi.org/10.1016/j.gloplacha.2012.06.007>
- Mészáros L, Dallos E, Vágó L, Czupi J, Paulik D, Darabos A, Marton T, Gy S, Ferenczy Z (1979) A Mihályi kutatási terület lehatároló fázisú zárójelentése, a szén-dioxid- és a „nem éghető” kevert gáztelepek vagyonszámítása. Hungarian Oil & Gas Company Plc, Budapest, p 116
- Nagymarosy A, Hámor G (2012) Genesis and evolution of Pannonian Basin. In: Haas J (ed) *Geology of Hungary, regional geology review*. Springer, Berlin, pp 149–200
- NOAA/ESRL (2019) Trends in atmospheric carbon dioxide. www.esrl.noaa.gov/gmd/ccgg/trends. Accessed 10 Dec 2019
- Palcsu L, Vető I, Futó I, Vodila G, Papp L, Major Z (2014) In-reservoir mixing of mantle-derived CO₂ and metasedimentary CH₄-N₂ fluids – noble gas and stable isotope study of two multistacked fields (Pannonian Basin System, W-Hungary). *Mar Pet Geol* 54:216–227. <https://doi.org/10.1016/j.marpetgeo.2014.03.013>
- Panisova J, Balázs A, Zs Z, Bielik M, Horváth F, Sz H, Schmidt S, Götze HJ (2017) Intraplate volcanism in the Danube Basin of NW Hungary: 3D geophysical modelling of the Late Miocene Pásztori volcano. *Int J Earth Sci* 107:1713–1730. <https://doi.org/10.1007/s00531-017-1567-5>
- Paris Agreement (2015) Paris Agreement to the United Nations Framework Convention on Climate Change, Dec. 12, 2015, T.I.A.S. No. 16–1104. https://unfccc.int/files/essential_background/convention/application/pdf/english_paris_agreement.pdf
- Pearce JM, Shepherd TJ, Kemp SJ, Wagner D, Rochelle CA, Bouch JE, Nador A, Vető I, Baker J, Toth G, Lombardi S, Annuziatellis A, Beaubien SE, Ciotoli G, Pauwels H, Chernichowski-Lauriol I, Gaus I, Le Nindre YM, Girard JP, Serra H, Petelet-Giraud E, Guern-Marot C, Orlic B, Schroot B, Schutteehelm A, Hatziyannis G, Spyridonos E, Metaxas A, Brune S, Hagendorf, J, Teschner M, Faber E, Poggenburg J, Illiffe J, Kroos BM, Alles A, Hildenbrand A, Heggland R (2005) Natural analogues for the geological storage of CO₂, NASCENT project. In: European Commission, Fifth Framework Research Programme, p 115
- Pogácsás G (1984) Seismic stratigraphic features of the neogene sediments in the Pannonian Basin. *Geophys Trans* 30:373–410
- Qi H, Coplen TB, Olack GA, Vennemann TW (2014) Caution on the use of NBS-30 biotite for hydrogen-isotope measurements with on-line high-temperature conversion systems. *Rapid Commun Mass Spectrom* 28:1987–1994
- Rauzi SL (1999) Carbon dioxide in the StJohns–Springville Area, Apache Country, Arizona. *Arizona Geol Surv Open-File Rep* 99–2:24
- Sacchi M, Horváth F (2002) Towards a new time scale for the Upper Miocene continental series of the Pannonian basin (Central Paratethys). *Eur Geosci Union, Stephan Mueller Spec Publ* 3:79–94. <https://doi.org/10.5194/smsps-3-79-2002>
- Savin SM, Epstein S (1970) The oxygen and hydrogen isotope geochemistry of clay minerals. *Geochim Cosmochim Acta* 34:43–63
- Schléder Z (2001) Pásztori környéki fűrészek miocén vulkánai közeteinek közettani és geokémiai vizsgálata. Phd thesis, Eötvös Lorand University, Budapest, Hungary, p 109
- Sharp ZD, Atudorei V, Durakiewicz T (2001) A rapid method for determination of hydrogen and oxygen isotope ratios from water and hydrous minerals. *Chem Geol* 178:197–210. [https://doi.org/10.1016/S0009-2541\(01\)00262-5](https://doi.org/10.1016/S0009-2541(01)00262-5)
- Suzuoki T, Epstein S (1976) Hydrogen isotope fractionation between OH-bearing minerals and water. *Geochim Cosmochim Acta* 40:1229–1240
- Sztanó O, Magyar I, Szónoky M, Lantos M, Müller P, Lenkey L, Katona L, Csillag G (2013) A Tihanyi Formáció a Balaton környékén: típusjelvény, képződési körülmények, rétegtani jellemzés. *Földtani Közlemények* 143(1):73–98
- Sztanó O, Kovač M, Magyar I, Suján M, Fodor L, Uhrin A, Rybár S, Csillag G, Tőkés L (2016) Late Miocene sedimentary record of the Danube/Kisalföld Basin: interregional correlation of depositional systems, stratigraphy and structural evolution. *Geol Carpath* 67(6):525–542. <https://doi.org/10.1515/geoca-2016-0033>
- Tari G (1994) Alpine Tectonics of the Pannonian Basin-PhD Thesis, Rice University, Houston, Texas, p 501
- Vakarcs G, Vail P, Tari G, Gy P, Mattick R, Szabó A (1994) Third-order Middle Miocene-Pliocene depositional sequences in the prograding delta complex of the Pannonian Basin. *Tectonophysics* 24:81–106. [https://doi.org/10.1016/0040-1951\(94\)90265-8](https://doi.org/10.1016/0040-1951(94)90265-8)
- Vető I, Csizmeg J, Cs S (2014) Mantle-related CO₂, metasedimentary HC-N₂ gas and oil traces in the Répcelak and Mihályi accumulations, W-Hungary—mixing of three fluids of very different origin. *Cent Eur Geol* 57(1):53–69. <https://doi.org/10.1556/CEuGeol.57.2014.1.3>
- Wang S, Kim J, Lee M (2016) Measurement of the scCO₂ storage ratio for the CO₂ reservoir rocks in Korea. *Energy Proced* 97:342–347. <https://doi.org/10.1016/j.egypro.2016.10.015>
- Watson MN, Zwingmann N, Lemon NM (2004) The Ladbroke Grove–Katnook carbon dioxide natural laboratory: a recent CO₂ accumulation in a lithic sandstone reservoir. *Energy* 29:1457–1466. <https://doi.org/10.1016/j.energy.2004.03.079>
- Worden RH (2006) Dawsonite cement in the Triassic Lam Formation, Shabwa Basin, Yemen: a natural analogue for a potential mineral product of subsurface CO₂ storage for greenhouse gas reduction. *Mar Pet Geol* 23:61–77. <https://doi.org/10.1016/j.marpetgeo.2005.07.001>
- Xu T, Apps JA, Pruess K (2003) Reactive geochemical transport simulation to study mineral trapping for CO₂ disposal in deep arenaceous formations. *J Geophys Res* 108:2071–2084. <https://doi.org/10.1029/2002JB001979>
- Zhou B, Liu L, Zhao S, Ming XR, Oelkers EH, Yu ZC, Zhu DF (2014) Dawsonite formation in the Beier Sag, Hailer Basin, NE China tuff: a natural analog for mineral carbon storage. *Appl Geochem* 48:155–167. <https://doi.org/10.1016/j.apgeochem.2014.07.015>
- Zilahi-Sebess L (2013) Országos geotermikus potenciál-felmérés eredményei. Új utak a földtudományban, Országos Kőolajipari Tröszt (in Hungarian)

Publisher's Note Springer Nature remains neutral with regard to jurisdictional claims in published maps and institutional affiliations.